

## 9. Jointed Rock Model

Natural soils and sedimentary rocks, such as shale, limestone and mudstone, are typically formed by deposition and progressive consolidation during formation. Such formations usually have a distinct internal structure, which is characterized by the appearance of multiple sedimentary layers. Besides the bedding planes, the geometric layout of networks of joints and other types of discontinuities in a rock mass are significant contributors to the complex behavior of such geomaterials (e.g., Hoek and Brown 1980, Hoek 1983, Zienkiewicz and Pande 1977). The presence of these fissures and planes of weakness significantly influences the response of geotechnical structures such as slopes, tunnels, and excavations (Goodman et al, 1968, Bandis et al, 1983). The jointed rock model can be used to handle these cases, where a network of discontinuities is to be isolated from the rock mass and their effects on the behavior considered explicitly.

The jointed rock mass is considered to be composed of matrix, such as an intact rock, that is intersected by up to three sets of weak planes (Azami et. al., 2012). The spacing of the weak planes is such that the overall effects of the sets can be smeared and averaged over the control volume of the material. Such a configuration with two sets of weak planes is illustrated in Figure 9.1 where the weak planes are oriented at an arbitrary angle  $\alpha_1$  and  $\alpha_2$  in the rock mass.

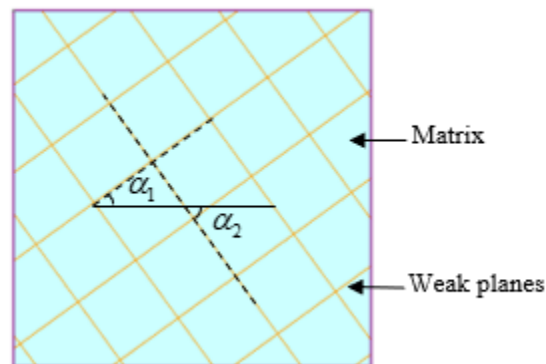


Figure 9.1. Typical control volume of a material with two sets of weak planes with inclination angle  $\alpha_1$  and  $\alpha_2$

The matrix can have elastic behavior, or its failure can be described by either a Mohr-Coulomb criterion or a Generalized Hoek-Brown criterion presented in equations 9.1 and 9.2 respectively.

$$F_s = \frac{1}{2}(\sigma_1 - \sigma_3) + \frac{1}{2}(\sigma_1 + \sigma_3) \sin \phi - c \cos \phi = 0 \quad (9.1)$$

$$F_s = \sigma_1 - \sigma_3 - \sigma_{ci} \left( m \frac{-\sigma_1}{\sigma_{ci}} + s \right)^a = 0 \quad (9.2)$$

The material model for the matrix is the same as what was presented in previous chapters for Mohr-Coulomb and Generalized Hoek-Brown models. That includes the options for plastic potential functions, the residual values for material parameters, and the tensile yield functions.

A tensile strength is also considered for the matrix by using a tension cut off yield surface and including a tensile strength in the material properties.

The strength criterion of the weak planes is formulated by Coulomb criterion, Barton-Bandis criterion or Geosynthetic Hyperbolic function, the formulations of which are presented in equations 9.3 to 9.5 respectively.

$$f = \tau + \sigma_n \tan \phi - c \quad (9.3)$$

$$f = \tau + \sigma_n \tan \left( \phi_r + JCR \log \left( \frac{JCS}{-\sigma_n} \right) \right) \quad (9.4)$$

$$\tau = - \frac{a_\infty \sigma_n \tan \phi_0}{a_\infty - \sigma_n \tan \phi_0} \quad (9.5)$$

In above  $\tau$  and  $\sigma_n$  are the shear and normal components of stress vector acting on the weak plane. The material properties for the Coulomb criterion are the friction angle,  $\phi$ , and cohesion,  $c$ . In Barton-Bandis criterion,  $\phi_r$  is the residual friction angle,  $JCR$  is the joint roughness coefficient,  $JCS$  and is the joint wall compressive strength (Barton, 1973, 1976). The material parameters in the hyperbolic function in equation 9.5 are adhesion,  $a_\infty$ , that defines the shear strength at infinite compression, and friction angle,  $\phi_0$ , that defines the friction angle at  $\sigma_n = 0$ .

The shear strength formulated by the three criteria above can accept peak and residual states. The plastic potential function for the weak planes has the same form as the failure function with a dilation angle replacing the friction angle in the corresponding function.

The effects of the weak planes are illustrated in Figures 9.1 and 9.2 that show the uniaxial compression strength of two jointed rocks. Figure 9.1 shows the variation of the uniaxial strength of a jointed rock that has one set of weak planes with the orientation of the weak planes. The numerical results are verified by a comparison to the analytical results. Figure 9.2 shows the same graphs for a rock that has two sets of perpendicular weak planes with same properties. The results presented here use a Mohr-Coulomb criteria for the intact rock with a friction angle of  $35^\circ$  and a cohesion equal to 100 kPa, the weak planes use a Coulomb criterion with a friction angle of  $30^\circ$  and a cohesion equal to 40 kPa.

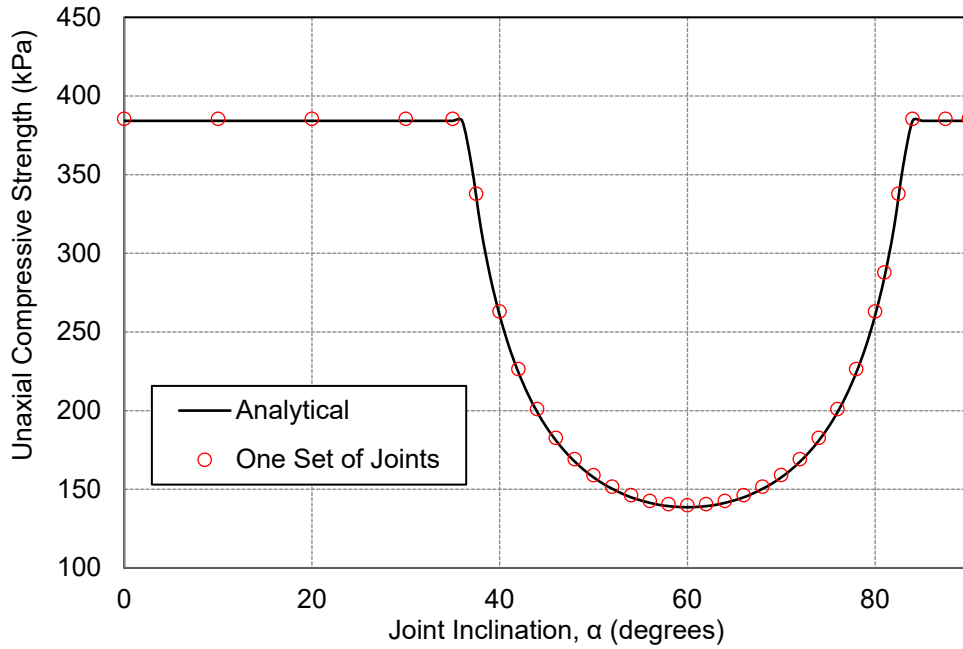


Figure 9.2. Variation of uniaxial compressive strength for one set of weak planes

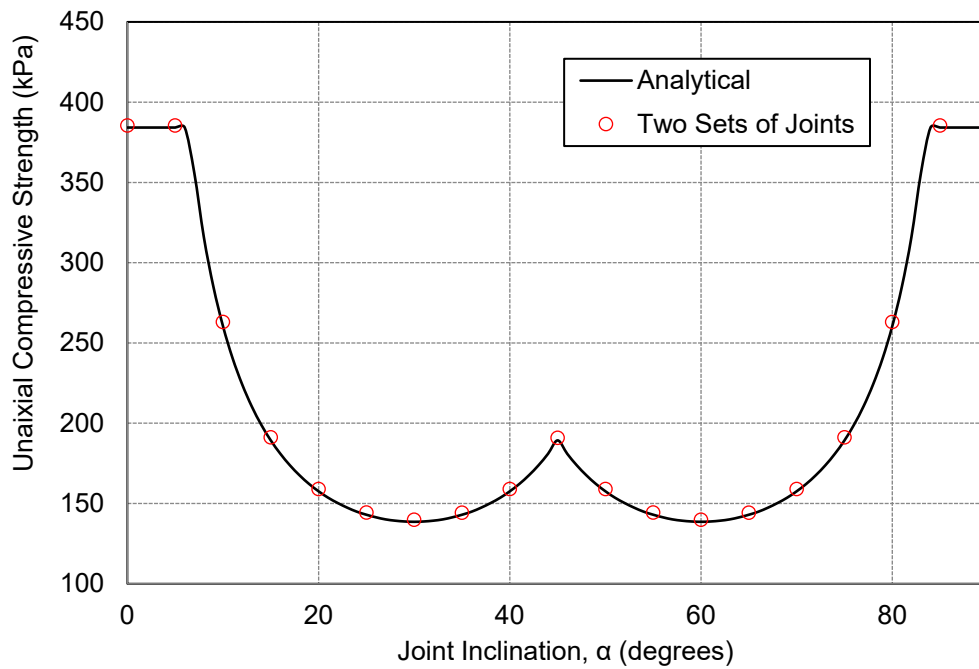


Figure 9.3. Variation of uniaxial compressive strength for two sets of weak planes

Tensile strength is another failure criterion for the weak planes.

$$f_T = \sigma_n - T = 0 \quad (9.6)$$

In above  $T$  is the tensile strength of the weak planes. The flow rule for tensile failure of weak planes is associated.

## References

- Azami A., Yacoub T. & Curran J., 2012. Effects of strength an-isotropy on the stability of slopes. 65th Canadian Geotechnical Conference, CGS Geo-Manitoba, Winnipeg, Manitoba, Canada.
- Bandis, S.C., Lumsden, A.C. and Barton, N.R., 1983. Fundamentals of rock joint deformation. International Journal of Rock Mechanics, Mining Sciences & Geomechanics Abstracts, 20(6): 249-268.
- Dawson, E.M., Roth, W.H. and Drescher, A. 1999 Slope stability analysis by strength reduction, Geotechnique, 49(6): 835-840.
- Goodman, R.E., Taylor, R.L. and Brekke, T.L., 1968. A model for the mechanics of jointed rock. Journal of the Soil Mechanics and Foundations Division, ASCE, 637-659.
- Hoek E. and Brown E.T. 1980. Underground Excavations in Rock. London, Instn Min. Metal, England.
- Hoek E. (1983), Strength of jointed rock masses. Geotechnique, Vol. 33, No. 3, 187-205.
- Zienkiewicz, O.C. and Pande G.N. 1977. Time-dependent multilaminar model of rocks-a numerical study of deformation and failure of rock masses, International Journal for Numerical and Analytical Methods in Geomechanics, 1(3): 219-247.